

University of Nebraska - Lincoln

DigitalCommons@University of Nebraska - Lincoln

David Sellmyer Publications

Research Papers in Physics and Astronomy

January 1987

Electronic structure, photoemission, and magnetism in Gd₂Co and Er₂Co glasses

Sitaram Jaswal

University of Nebraska, sjaswal1@unl.edu

David J. Sellmyer

University of Nebraska-Lincoln, dsellmyer@unl.edu

M. Engelhardt

University of Nebraska - Lincoln

Z. Zhao

University of Nebraska - Lincoln

A.J. Arko

Argonne National Laboratory, Argonne, Illinois

See next page for additional authors

Follow this and additional works at: <https://digitalcommons.unl.edu/physicssellmyer>



Part of the [Physics Commons](#)

Jaswal, Sitaram; Sellmyer, David J.; Engelhardt, M.; Zhao, Z.; Arko, A.J.; and Xie, K., "Electronic structure, photoemission, and magnetism in Gd₂Co and Er₂Co glasses" (1987). *David Sellmyer Publications*. 142.
<https://digitalcommons.unl.edu/physicssellmyer/142>

This Article is brought to you for free and open access by the Research Papers in Physics and Astronomy at DigitalCommons@University of Nebraska - Lincoln. It has been accepted for inclusion in David Sellmyer Publications by an authorized administrator of DigitalCommons@University of Nebraska - Lincoln.

Authors

Sitaram Jaswal, David J. Sellmyer, M. Engelhardt, Z. Zhao, A.J. Arko, and K. Xie

Electronic structure, photoemission, and magnetism in Gd_2Co and Er_2Co glasses

S. S. Jaswal, D. J. Sellmyer, M. Engelhardt, and Z. Zhao

Behlen Laboratory of Physics, University of Nebraska, Lincoln, Nebraska 68588-0111

A. J. Arko

Argonne National Laboratory, Argonne, Illinois 60439

K. Xie

Institute of Physics, Chinese Academy of Sciences, Beijing, China

(Received 12 June 1986)

The electronic and magnetic structures of amorphous Gd_2Co and Er_2Co are studied by ultraviolet and x-ray photoemission measurements and band calculations. The spectra for both glasses show a band of Co $3d$ levels centered at a binding energy E_B of about -1.0 eV and peaks arising from $4f$ levels at $E_B = -8.4$ eV and $E_B \cong -5-9$ eV for Gd and Er, respectively. Magnetization data have shown that $a\text{-Gd}_2\text{Co}$ possesses a ferrimagnetic structure with a small Co moment. The linear-muffin-tin-orbital method is used to perform self-consistent, spin-polarized calculations in the semirelativistic approximation for Gd_2Co . Because of the complexity of the glassy structure, the calculations are performed for body-centered-tetragonal and cubic fluorite structures, and the sensitivity to local environment effects studied. The calculations are in a good overall agreement with the photoemission and magnetic-moment results.

I. INTRODUCTION

Our understanding of the electronic structure of rare-earth-transition-metal glasses, and its relation to magnetic and optical properties, is in a rudimentary state. This is true for several reasons. Experimentally, the rare-earth metals are notoriously reactive so that it is difficult to prepare and maintain pure surfaces for photoemission measurements. Theoretically there are two significant problems. One is the general problem associated with solving the Schrödinger equation without the aid of Bloch's theorem. The other is computational difficulties inherent in achieving self-consistency when treating tightly bound $4f$ states near the Fermi level. Relativistic effects and the necessity to do spin-polarized calculations in these magnetically ordered materials are additional complications that prevent all but the intrepid from studying this class of materials.

In spite of these difficulties, there is considerable intrinsic interest in RE-TM glasses. In part this stems from the circumstance that there are huge numbers of glass-forming combinations which result from the well-known similarity of the RE-TM phase diagrams, when one RE metal is substituted for another. A second driving force is the high potential for information storage devices based on RE-TM glasses. It is likely that erasable magneto-optic media, perpendicular recording materials, and bubble memory devices all will include such materials in systems to be developed in the future.¹ Clearly, for such applications there is much to be learned about the interplay between electronic structure, optical properties, magnetism, and other chemical and structural properties.

Because of the paucity of research on the electronic structure of RE-TM glasses, previous studies on them can

be summarized with brevity. Güntherodt and Shevchik performed x-ray photoemission spectroscopy (XPS) measurements on amorphous alloys of the form $a\text{-Gd}_x\text{Fe}_{1-x}$ ($0 \leq x \leq 1$).² The resulting valence-band spectra could be described approximately as a linear superposition of those of the pure elements. A small $\text{Gd} \rightarrow \text{Fe}$ and $\text{Fe } s \rightarrow d$ charge transfer was deduced from an unchanged Fe $2p$ core-level line-shape asymmetry and small shifts in the Gd and Fe core levels. This charge transfer is smaller than that in Gd-Fe intermetallic phases, but it was unclear how a small charge transfer could be reconciled with a reduction in the Fe moment from $2.2\mu_B$ in crystalline Fe ($c\text{-Fe}$) to $1.55\mu_B$ for $c\text{-GdFe}_2$ and $a\text{-GdFe}_2$. Terzieff and Lee³ studied $4f$ and core-level spectra in $a\text{-Gd}_x\text{Fe}_{1-x}$ and $a\text{-Gd}_x\text{Co}_{1-x}$ alloys, for $x \leq 0.34$. From the similarity of the XPS binding energies in the pure elements and glasses, it was concluded that the $\text{Gd} \rightarrow \text{Fe}$ charge transfer, if existing at all, must be less than one electron per Gd atom. This is smaller than the values of 1.41 and 1.86 electrons per Gd atom calculated from magnetization measurements and a mean-field calculation for $a\text{-GdCo}$, respectively. These authors also characterized the influence on the Gd $4d$ and $4f$ of oxidation of the sample surface.

The electronic density of states for both the filled and unfilled states of $a\text{-Y}_{0.21}\text{Fe}_{0.79}$ and $a\text{-Tb}_{0.21}\text{Fe}_{0.79}$ have been studied with XPS and inverse XPS by Connell *et al.*⁴ In this work it was possible to develop an Fe d -band model consisting of majority and minority spin bands exchange split by 1.8 eV. This model is consistent with the photoemission results and also was compared in a subsequent paper with the optical and magneto-optical properties of $a\text{-TbFe}$. Thus a correlation was made between fundamental electronic structure of this magnetic glass and the magnitude of the Kerr effect, the physical basis for

magneto-optical storage materials.

Currently, there have been no attempts to perform theoretical calculations on realistic models of RE-TM glasses. Oelhafen has given a review of results on electron spectroscopy of metallic glasses, primarily intertransition-metal and TM-metalloid glasses.⁵ Recent theoretical calculations on such alloys have shown significant progress for glasses such as *a*-ZrCu, *a*-ZrNi, *a*-ZrPd, and others.⁶ But, for reasons mentioned earlier, RE-TM glasses have not been studied theoretically as yet.

In this paper we report photoemission measurements on *a*-Gd₂Co and *a*-Er₂Co and on self-consistent, spin-polarized electronic structure calculations on simple structural models of Gd₂Co. Earlier work in our laboratory showed that the Gd glass orders ferrimagnetically at $T_c = 170$ K and the Er glass orders sperimagnetically at $T_c = 12$ K.⁷ The latter ordering refers to the situation where the Er moments are spread into a cone or fanlike arrangement whose origin is a strong single-ion anisotropy on the Er ions.⁸ The axis of this cone is opposed to the Co subnetwork moment because of the well-known antiparallel coupling of transition-metal moments with those of heavy rare-earth moments. The size of the Co moment in *a*-GdCo alloys has been considered by several authors, but most recently by Fukamichi *et al.*,⁹ who reviewed earlier work. This aspect is clearly related to the charge transfer and electronic structure. Thus, one of the aims of this work was to determine the extent to which present state-of-the-art calculational methods could describe both the photoemission and magnetic properties of this relatively complex class of solids.

II. PHOTOEMISSION EXPERIMENTS

The alloys were performed by first arc melting the pure constituents several times. Then a small button (~ 0.1 g) of the alloy was rapidly quenched from the melt with a quench rate estimated to be $\sim 10^6$ K/s. This produced foils of about 3 cm in diameter and 50 μ m in thickness which were shown to be amorphous by x-ray diffraction measurements. Both ultraviolet photoemission spectroscopy (UPS) and x-ray photoemission spectroscopy (XPS) measurements were performed, the former with tunable radiation obtained from the Tantalus Storage Ring at the University of Wisconsin. The UPS studies employed a Vacuum Generators ADES 400 system in combination with a 2-m grazing incidence monochrometer that provided photons from about 40 to 120 eV. The resolution of the monochrometer was about 0.3 eV at 40 eV and rose to about 1 eV at 100 eV. In addition, the analyzer was operated in a fixed pass energy mode with a resolution of about 0.3 eV. The limited XPS measurements were performed on a Vacuum Generators ESCALAB 5 instrument with a resolution of about 0.5 eV.

Figure 1 illustrates the difficulty encountered in attempting to clean the surface of a RE-TM glass. Cleaning was performed *in situ* by repeated 2-kV Ne-ion bombardments, followed by the pumpout of the Ne gas and the taking of a UPS spectrum. Figure 1 shows the results on *a*-Gd₆₅Co₃₅ after 5, 50, and 111 min of sputter cleaning. The oxygen peak at a binding energy of ~ -6 eV,

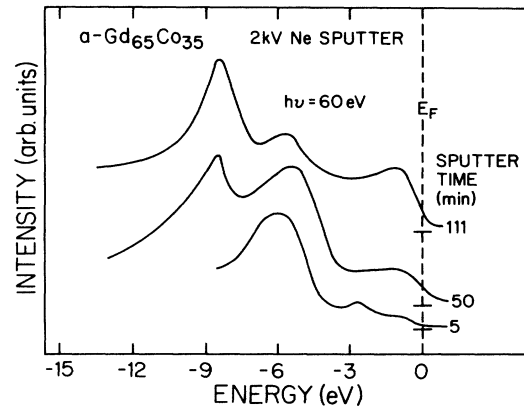


FIG. 1. UPS spectra of *a*-Gd₆₅Co₃₅ after varying sputter-cleaning treatments.

while clearly diminishing with time, seemed to approach an asymptotic limit as shown for the 111-min sputtering. That is, we were unable to completely eliminate this feature even with much longer sputter cleaning periods. We speculate that this follows either from some residual oxygen absorbed in the bulk of the sample, or from a surface layer formed during the approximate 5-min period during which the Ne gas was pumped out of the chamber. During these experiments, Auger-electron spectroscopy was not available as a test for surface cleanliness. However, this turned out not to be significant because we were limited in our ability to obtain a perfectly clean surface in any case. Thus, in all the measurements we report we avoid any discussion of valence-band structure in the vicinity of $E_F \approx -6$ eV. Fortunately, the major structure of the 4*f* and 3*d* bands is either at higher or lower binding energies than -6 eV, so the cleanliness problem is minimized.

Figure 2 shows the 60-eV spectrum of *a*-Er₆₅Co₃₅, along with earlier UPS *c*-Co (Ref. 10) and XPS *c*-Er (Ref. 11) spectra. Several features should be noted here.

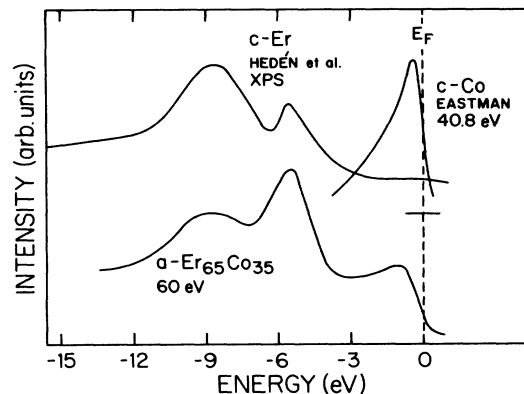


FIG. 2. 60-eV spectrum of *a*-Er₆₅Co₃₅ and comparison with *c*-Er and *c*-Co (see Refs. 10 and 11).

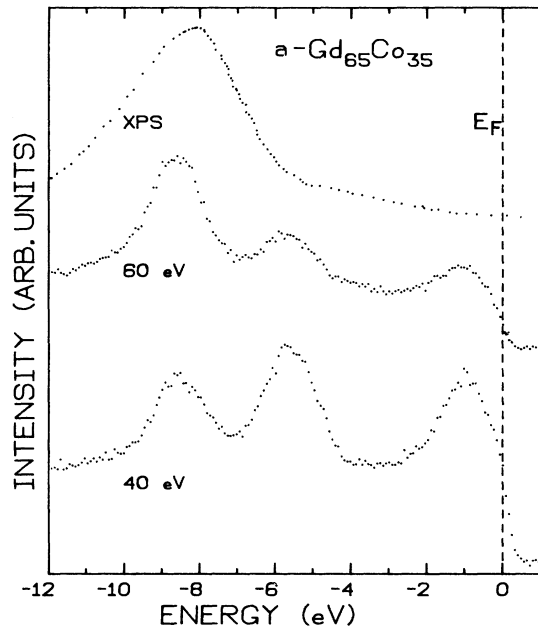


FIG. 3. 40-eV, 60-eV, and XPS data on $a\text{-Gd}_{65}\text{Co}_{35}$.

One is that the Er 4*f* levels are separated into a relatively broad group of multiplet levels centered on about -9 eV and a smaller set at about -6 eV. Judging from the relative intensities of the -9 and -6 eV peaks in the $a\text{-ErCo}$ spectrum, there is likely to be a contribution to the -6 eV peak from oxygen in this spectrum as well. A second point is that the peak at -1 eV in the $a\text{-ErCo}$ spectrum clearly should be associated mainly with Co 3*d* states. The position of the Co 3*d* peak (~ -1.0 eV) appears to be shifted to higher binding energies than in pure Co. This point has been discussed by Oelhafen⁵ for several other glasses containing TM elements, and has been related to the high glass-forming ability and stability of these materials.

UPS spectra at 40 and 60 eV and an XPS spectrum for $a\text{-GdCo}$ are shown in Fig. 3. Features of interest here are the Gd 4*f* level at ~ -8.5 eV and the Co 3*d* levels concentrated within 2–3 eV on E_F . Also it is seen that higher photon energies emphasize the structure at higher binding energies to the extent that there is very little Co 3*d* intensity left near E_F in the XPS spectrum. It can be noticed that the 4*f* peak centers on about -8.5 eV in the UPS spectrum but has its maximum at about -8.1 eV in the XPS spectrum. It is not entirely clear whether this slight shift is related to the different photon energies or to a slight effect of oxide formation on the surface. Terzieff and Lee noted for pure Gd that a deliberate oxidation of the surface produced a shift of the 4*f* peak from -7.9 to -8.9 eV.³ Finally, as in the $a\text{-ErCo}$ case, there seems to be a clear shift of the Co peak from about 0 in pure Co to about -1 eV in the glass.

III. ELECTRONIC STRUCTURE CALCULATIONS

Self-consistent spin-polarized electronic structure calculations for elemental Gd metal are known to converge

very slowly due to the relatively sharp unoccupied spin-down *f* band near the Fermi level. A similar circumstance makes such calculations for a realistic atomic model (a very large cluster) of Gd_2Co glass extremely difficult and time consuming. Therefore we simulate the glass here with two crystalline structures of the same composition and the average mass density as that of the glass. The calculations are performed on a fairly symmetric CaF_2 structure and a body-centered-tetragonal (BCT) structure of somewhat lower symmetry. Comparison of the results for the two structures should give us an indication of the influence of the short-range order on the electron structure of the glass. In principle, one could get a fairly good representation of the electronic structure of the glass by averaging the results for a large number of different crystalline structures.

The self-consistent spin-polarized calculations are based on the linear-muffin-tin-orbital (LMTO) method¹² in the semirelativistic approximation. The Hedin–von Barth form¹³ of the local-spin-density approximation to the exchange correlation potential with Janak parameters¹⁴ was used in these calculations. The core states for Gd ($1s^2 2s^2 2p^6 3s^2 3p^6 3d^{10} 4s^2 4p^6 4d^{10} 5s^2 5p^6$) and Co ($1s^2 2s^2 2p^6 3s^2 3p^6$) were frozen to be the same as the atomic states found self-consistently. The Wigner-Seitz sphere radii used for Gd and Co are 2.603 and 3.738 a.u., respectively. The self-consistent solutions in the solid were found for the *s*, *p*, *d*, and *f* valence states. The atomic sphere approximation and the neglect of higher partial waves are corrected to first order in energy

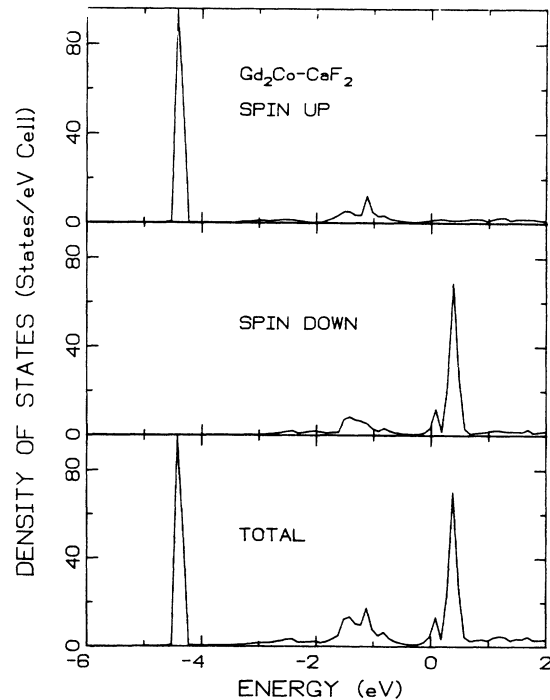


FIG. 4. Spin-polarized density-of-states calculations for Gd_2Co in the CaF_2 structure.

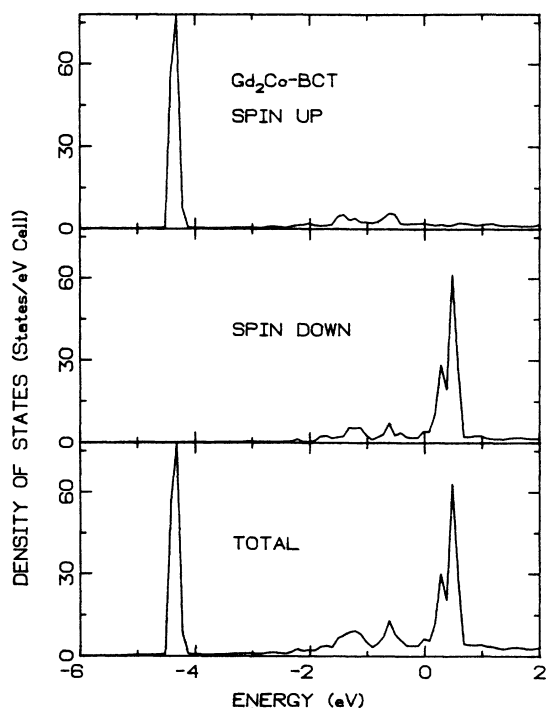


FIG. 5. Spin-polarized density-of-states calculations for Gd_2Co in the BCT structure.

through the combined correction term. We were unable to use the fast self-consistently procedure based on scaling due to the sharp $4f$ Gd band near the Fermi level. About 30 iterations of the standard slower self-consistency procedure were required for each structure. The LMTO programs used here are basically those described in Ref. 15.

The densities of states (DOS) for the two structures are shown in Figs. 4 and 5. The DOS consists of highly localized f bands due to Gd and partially localized d bands due to Co. The Gd f bands in the two structures are quite similar with the occupied band being about 4.5 eV below the Fermi level and the unoccupied band being about 0.5 eV above the Fermi level. This result is very similar to that of Gd metal.^{16,17} Thus, the f band is expected to be fairly independent of the short-range order in a solid. The Co d band is just below the Fermi level for both the spin-up and spin-down states. The general shapes of the Co d bands for the two structures are similar with a few differences in the fine structure. There is no evidence in the Co d states for any simple exchange splitting between the opposite spin bands. There is a small charge transfer from Co to the two Gd atoms ($0.56e$ in the CaF_2 structure and $0.21e$ in the BCT structure). Since the localized and extended states respond differently to the incident photons, they are considered separately in the discussion below.

A. Co d band

Because of the extended nature of the d states, Koopman's theorem should be reasonable for the Co d band. Therefore, one can directly compare the calculated

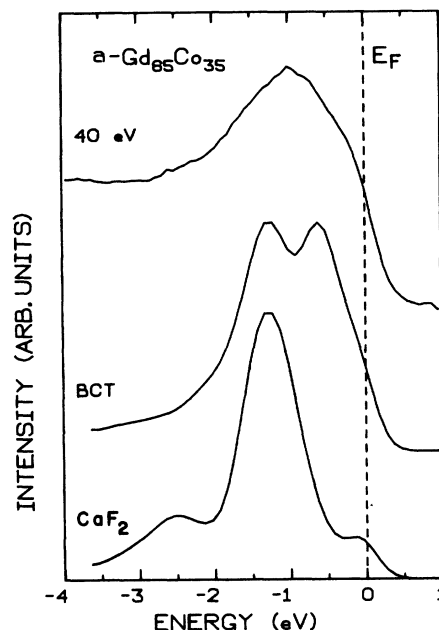


FIG. 6. Comparison of the Co $3d$ levels in the 40 eV UPS spectra with the calculated DOS for the two structures. The DOS curves have been broadened with a Gaussian function with a standard deviation of 0.2 eV.

one-electron eigenvalues with the photoemission data. The total densities of states for the Co d band with a Gaussian broadening of 0.2 eV are compared with the corresponding photoemission data with 40-eV photons in Fig. 6. We see that the Co d band is sensitive to the short order for the two structures and the glass can be gained by looking at the nearest-neighbor distances in Table I. The glass is expected to have a distribution of nearest-neighbor distances with peaks around 2.5, 3.58, and 3.04 Å for Co-Co, Gd-Gd, and Co-Gd, respectively. These distances are in qualitative agreement with the corresponding nearest-neighbor distances in the crystalline structures except for the Co-Co distance. The nearest-neighbor Co-Co distances in BCT (3.2 Å) and CaF_2 (4.74 Å) are much larger than the average Co-Co distance (2.5 Å) expected in the glass. Since the d - d hybridization decreases with increasing distances between the Co atoms, this is reflected in the differences between the various d bands in Fig. 6. Since the Co-Co distance is largest in the CaF_2 structure, its d band is the narrowest of all. As the Co-Co distance decreases in going from CaF_2 to BCT to

TABLE I. Nearest-neighbor distances in crystalline Co, Gd, and Gd_2Co (BCT and CaF_2 structures) in Å.

	Gd_2Co		Co	Gd	Co + Gd
	BCT	CaF_2			
Co-Co	3.2	4.74	2.50		
Gd-Gd	3.76	3.35		3.58	
Gd-Co	3.16	2.90			3.04

glassy structure, the d band broadens. Also the hybridization produces a two-peak structure due to a unique nearest-neighbor Co-Co distance in the BCT crystal whereas the Co photoemission band is expected to be smooth due to a distribution of the corresponding distances in the glass. If one averages the calculated results for the two structures, the theory and the experiment are in reasonably good agreement with each other. In particular, the calculations suggest a peak centered roughly at $E_B \cong -1$ eV, a feature clearly seen in the experimental results.

B. Gd f band

Because of the highly localized nature of Gd f states, Koopman's theorem is no longer applicable to them, and hence the calculated one-electron eigenvalues cannot be directly compared with the photoemission data. In order to study the photoemission of f electrons, one must calculate the change in the total energy of the system in this process by a Slater transition-state analysis.¹⁸ The change in the energy is given by

$$\Delta E = \int_{n_i}^{n_f} \frac{\delta E}{\delta n} \delta n = \int_{n_i}^{n_i-1} \epsilon \delta n,$$

where n_i and n_f are the initial and final occupation numbers and ϵ is the eigenvalue corresponding to the occupation n .¹⁹ It has been found that a linear dependence of ϵ on n is quite reasonable.²⁰ With this assumption

$$\begin{aligned} \Delta E &= - \left[\frac{\epsilon_{n_i} + \epsilon_{n_i-1}}{2} \right] = -\epsilon_{n_i} + \left[\frac{\epsilon_{n_i} - \epsilon_{n_i-1}}{2} \right] \\ &= -\epsilon_{n_i} + \delta. \end{aligned}$$

The second term is the correction to the Koopman's theorem. ϵ_{n_i} and ϵ_{n_i-1} are the Gd f -band positions for $4f^7$ and $4f^6$ configurations. In principle, one should use the supercell method to calculate the eigenvalue corresponding to $4f^6$ configuration.²¹ Because of the highly localized nature of the $4f$ electrons in Gd, a much simpler atomic calculation should give reasonable results. We have calculated ϵ_{n_i} and ϵ_{n_i-1} for the Gd atom with configurations $4f^7 5d^1 6s^2$ and $4f^6 5d^2 6s^2$, respectively. The change $5d^1 \rightarrow 5d^2$ is to simulate the local screening of the

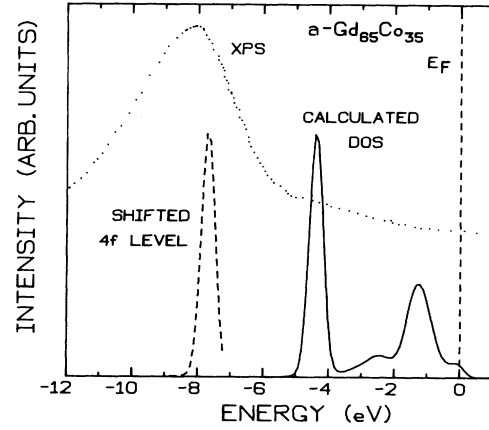


FIG. 7. Comparison of the experimental (dotted) and calculated (dashed) Gd $4f$ level for Gd_2Co (see text).

f hole in the solid. The calculations give $\delta = 3.3$ eV. The calculated f -band position in photoemission as determined by δ is indicated by a dotted line in Fig. 7 and is in very good agreement with the XPS data also plotted in the same figure. This result is similar to that of Herbst *et al.*²² based on renormalized atom scheme even though their Hartree-Fock $4f$ eigenvalue (about -16 eV) is much different from the more accurate value obtained by us and others^{15,16} (about -4.5 eV).

IV. MAGNETIC STRUCTURE

Experimental results on a - $Gd_{65}Co_{35}$ show that the ordered magnetic structure is ferrimagnetic and that the spontaneous moment is 195 ± 1 emu/g which corresponds to $4.4\mu_B$ per average atom. The apportioning of this moment among the various Gd and Co orbital states (s, p, d, f) is rather difficult and often simplifying assumptions are made such as taking the total moment associated with the Gd^{3+} ion to be $gJ = 7.0$. This ignores any Gd conduction-electron polarization but it is not easy, in an alloy, to measure the individual contributions. Fukamichi *et al.*⁹ have presented and reviewed the evidence relevant to the Gd and Co moments in a -GdCo alloys. Based on bulk magnetization, pressure derivative of T_c , and NMR

TABLE II. Comparison of calculated and experimental Gd and Co magnetic moments μ in μ_B .

	Gd		Co		Gd ₂ Co ^a	
	BCT	CaF ₂	BCT	CaF ₂	BCT	CaF ₂
	Calc.					
$s+p$	0.11	0.10	0.00	0.00	0.07	0.07
d	0.25	0.24	0.00	-0.21	0.17	0.09
f	6.74	6.71	0.00	0.00	4.49	4.47
Total	7.10	7.05	0.00	-0.21	4.73	4.63
	Expt. ^b					
	7.5		-0.6		4.4	

^aThese values represent moments per average atom.

^bData obtained from several experiments as discussed by Fukamichi *et al.*, Ref. 9.

data the best estimates for the moments of Gd, Co, and "average" atoms are 7.5, -0.6 , and 4.4 in units of μ_B , respectively. These data, along with the calculated results are shown in Table II. Several points of interest are the following. (a) The localized Gd $4f$ moment is not $7.0\mu_B$ but rather about $6.7\mu_B$ in the calculation. This results from an overlap of the tail of the unoccupied $4f$ level with E_F . (b) The calculation for the CaF_2 structure appears to better agree with experiment in the sense that it does predict a small moment (-0.21) on the Co atom which is antiparallel with the Gd moments. (c) There is reasonably good agreement between the calculated and measured average moments per atom, 4.6 – 4.7 and 4.4 , respectively. Given the apparent sensitivity of the Co moment to structure, it is clear that it will be very hard to calculate a more precise magnetic moment for the Gd and Co moments for a true glassy structure. That is, it is likely that the smooth variation in $\mu(\text{Co})$ plotted by Fukamichi *et al.*⁹ is a reflection of differing magnetic moments which depend sensitively on local atomic arrangements. This is surely a limitation on the calculation of detailed magnetic properties imposed by the inability to handle a realistic glassy structure with localized and spin-polarized f and d electrons.

V. SUMMARY AND CONCLUSIONS

The major results and conclusions on this work are as follows.

(1) UPS and XPS measurements on a -GdCo and a -ErCo alloys have shown that the rare-earth $4f$ levels are essentially unshifted from their positions in the pure metals. This is not unexpected given the localized nature of these states.

(2) In both glasses the Co $3d$ levels appears within about 3 eV of E_F , and there appears to be an increase in

the binding energy of these levels in comparison with elemental Co. This shift may be related to the relative ease of glass formation of this class of RE-TM glasses.

(3) Self-consistent spin-polarized electronic structure calculations were performed for two structural models of Gd_2Co . These calculations are in reasonably good agreement with the photoemission and magnetic-structure data. However, it was seen that only semiquantitative agreement with the Co valence-band structure and magnetic moment is attainable, and it will be very difficult to go beyond this because of the complexity of the glassy structure and the difficulty of the calculations.

(4) It was shown that one must go beyond Koopman's theorem and use a transition-state analysis to explain the position of the localized Gd $4f$ photoemission level in a -GdCo.

In general, the calculations show both localized and band features associated with the magnetism in these materials. Such calculations are sufficiently reliable in a quantitative sense that they may be applicable to other RE-TM glasses where optical and other properties are of interest for possible applications.

ACKNOWLEDGMENTS

We are grateful for financial support at the University of Nebraska from the National Science Foundation under Grants No. DMR 8110520 and No. INT 8419546, and at Argonne National Laboratory from the Department of Energy. We are indebted to the staff of the Synchrotron Radiation Center, University of Wisconsin, where some of the research was performed, for their hospitality. We are thankful to Hans Skriver for the LMTO programs and Bruce Harmon for the atomic programs. Finally, we appreciate many helpful discussions with Dale Koelling.

¹G. A. N. Connell, J. Magn. Magn. Mater. **54-57**, 1561 (1986).

²G. Güntherodt and N. J. Shevchik, *Magnetism and Magnetic Materials*, Proceedings of the 21st Annual Conference on Magnetism and Magnetic Materials, AIP Conf Proc. No. 29, edited by J. J. Becker, G. H. Lander, and J. J. Rhyne (AIP, New York, 1976).

³P. Terzieff and K. Lee, J. Appl. Phys. **50**, 3565 (1979).

⁴G. A. N. Connell, S. J. Oh, J. Allan, and R. Allan, J. Non-Cryst. Solids **61-62**, 1061 (1984).

⁵P. Oelhafen, in *Glassy Metals II*, Vol. 53 of *Topics in Applied Physics*, edited by H.-J. Güntherodt and H. Beck (Springer, New York, 1983), p. 283.

⁶S. S. Jaswal and W. Y. Ching, J. Non-Cryst. Solids **61-62**, 1273 (1984); W. Y. Ching, L. W. Song, and S. S. Jaswal, Phys. Rev. B **30**, 544 (1984); S. S. Jaswal, J. Non-Cryst. Solids **75**, 373 (1985).

⁷J. A. Gerber, D. J. Miller, and D. J. Sellmyer, J. Appl. Phys. **49**, 1699 (1978).

⁸For a recent review see, D. J. Sellmyer and S. Nafis, J. Appl. Phys. **57**, 3584 (1985).

⁹K. Fukamichi, K. Shirakawa, Y. Satoh, T. Masumoto, and T. Kaneko, J. Magn. Magn. Mater. **54-57**, 231 (1986).

¹⁰D. E. Eastman, J. Phys. (Paris) Colloq. **32**, C1-293 (1971).

¹¹P. O. Hedén, H. Lofgren, and S. B. M. Hagstrom, Phys. Rev. Lett. **26**, 432 (1971).

¹²O. K. Andersen, Phys. Rev. B **12**, 3060 (1975).

¹³L. Hedin and U. von Barth, J. Phys. C **5**, 1629 (1972).

¹⁴J. F. Janak, Phys. Rev. B **12**, 1257 (1975).

¹⁵H. L. Skriver, *The LMTO Method: Muffin Tin Orbitals and Electronic Structure* (Springer, Berlin, 1984).

¹⁶B. N. Harmon, J. Phys. (Paris) Colloq. **40**, C5-65 (1979).

¹⁷J. Sticht and J. Kübler, Solid State Commun. **53**, 529 (1985).

¹⁸J. C. Slater, Adv. Quantum Chem. **6**, 1 (1972).

¹⁹J. F. Janak, Phys. Rev. B **18**, 7165 (1978).

²⁰D. D. Koelling, Rep. Prog. Phys. **44**, 139 (1981).

²¹M. R. Norman, D. D. Koelling, and A. J. Freeman, Phys. Rev. B **31**, 6251 (1985).

²²J. F. Herbst, D. N. Lowy, and R. E. Watson, Phys. Rev. B **6**, 1913 (1972).